


A bio-based hyperbranched flame retardant towards the fire-safety and smoke-suppression epoxy composite

Zhiqian Lin^{1#}, Wangbin Zhang^{1#}, Gaobo Lou^{1,2}, Zhicheng Bai¹, Jinjia Xu¹, Hufeng Li¹, Yuhan Zong¹, Fengqing Chen^{1,2*} , Pingan Song^{3,4}, Lina Liu^{1,2} and Jinfeng Dai^{1,2*}

¹ School of Chemistry and Materials Engineering, Zhejiang A&F University, Hangzhou 311300, China

² Key Laboratory of Wood Science and Technology of Zhejiang Province, Zhejiang A&F University, Hangzhou 311300, China

³ Centre for Future Materials, University of Southern Queensland, Springfield QLD 4300, Australia

⁴ School of Agriculture and Environmental Science, University of Southern Queensland, Toowoomba, QLD 4305, Australia

[#] These authors contributed equally: Zhiqian Lin, Wangbin Zhang

* Corresponding authors, E-mail: fengqingchen@zafu.edu.cn; jinfengdai0601@gmail.com

Abstract

The design of fully biological flame retardants is vital for environment-friendly and sustainability development. Herein, a fully biological hyperbranched flame retardant named PA-DAD was synthesized successfully through a simple neutralization reaction between 1,10-Diaminodecane (DAD) and phytic acid (PA). PA-DAD as a kind of reactive flame retardant was subsequently employed to composite with epoxy resin (EP). The obtained EP composite, comprising 25 wt% PA-DAD, exhibited excellent flame resistance with an appreciative limiting oxygen index (LOI) of 28.0%, and a desired V-0 rating of UL-94. The favorable attributes stem from the evident flame-retardant characteristics of PA-DAD, manifesting particularly within the gaseous and condensed phases of combustion. Benefitting from the PA-DAD with the synergistic effect of smoke suppression and flame resistance, the EP/25% PA-DAD composite displayed highlighted reductions both in smoke production and heat release rate. In contrast with neat EP, total smoke production (TSP), peak smoke production release (pSPR), the peak heat release rate (pHRR), and the rate of fire growth (FIGRA) of the EP/25% PA-DAD composite were decreased by 49.5%, 57.0%, 72.2% and 77.8%, respectively. Moreover, the EP/25% PA-DAD composite resulted in well-preserved mechanical properties, especially enhanced toughness, compared with the neat EP. The strategies in our work provided a facile, green, and highly efficient way for fabricating high fire-retardant EP composites.

Citation: Lin Z, Zhang W, Lou G, Bai Z, Xu J, et al. 2023. A bio-based hyperbranched flame retardant towards the fire-safety and smoke-suppression epoxy composite. *Emergency Management Science and Technology* 3:21 <https://doi.org/10.48130/EMST-2023-0021>

Introduction

Epoxy resin (EP) plays a vital role in human daily life, which has been employed in different areas of adhesives, coatings, insulation materials, and structural composites for its outstanding chemical resistance, adhesion, high mechanical properties, and electrical insulation^[1–6]. However, the highly intrinsic flammability and dense smoke of EP during combustion poses some threats to human safety and property^[7–11]. The modification of flame retardancy for EP is imperative and indispensable^[12–14]. In this regard, many strategies have been developed to improve flame retardancy of EP composites. Incorporation of flame retardants (FRs) into polymeric matrix is generally one of the most efficient and economical ways to pursue excellent flame retardancy for EP^[15,16]. Thus, numerous FRs have been designed to hinder fire hazards of polymers in the past decades^[17–21]. Nevertheless, a significant proportion of FRs for the EP matrix are originated from non-renewable petrochemical sources, which goes against the principles of global sustainability and environmental biodegradability. On this account, biological flame retardants have been attracting increasing attention for their inherent renewability, abundance, and biodegradability^[22–28].

So far, numerous bio-based FRs have been prepared and investigated for imparting flame retardancy to EP, such as lignin^[29], cardano^[30,31], eugenol^[32], phytic acid^[33–35], itaconic acid^[36], resveratrol^[37] and cyclodextrin^[38,39], and so on. Among

them, phytic acid (PA) possesses high flame-retardant efficiency because of its high phosphorus content of 28 wt%. PA is a phosphorus-rich organic acid, derived from the seeds and roots of the plant, which could provide an acid source for intumescent FRs^[40,41]. Wang et al.^[35] prepared a nano-layered hybrid as a kind of intumescent flame retardant for EP by a neutralization reaction of melamine and PA, and the obtained composites showed both good smoke suppression and flame resistance. Fang et al.^[33] improved the flame resistance of EP *via* synthesizing one unique phosphorus compound by the neutralization of phenyl phosphonate and PA, affecting condensed and gas phases. Zhu et al.^[34] synthesized a macromolecule ammonium phytic acid *via* a neutralization reaction of PA and N-aminoethyl piperazine for reducing smoke emissions and enhancing flame retardancy as a curing agent for EP. However, it is noted that the amines chelated with PA reported in the literature were petroleum-based products, which did not achieve all bio-based FRs.

In this work, a fully biological flame retardant (PA-DAD) was designed *via* a neutralization reaction between 1,10-diaminodecane (DAD) and PA that from renewable castor oil. The resulting PA-DAD exhibited both favourable smoke suppression and flame retardancy due to the generated bi-phase effect from PA-DAD in EP composites. The existing mechanism of flame retardancy for PA-DAD was explored using SEM-EDS, TG-IR, and Py-GC/MS methods. The transferring for heat and

oxygen can be declined by the formed compact char, protecting the residual matrix from additional thermal degradation and decreasing emissions of toxic gases. The mechanical performances of EP/PA-DAD composites with a satisfactory toughness were methodically investigated. PA-DAD was demonstrated as a high-efficient green smoke suppressant as well as flame retardant for EP, expecting to contribute to low-carbon programs.

Experiments and methods

Materials

Dicyandiamide (DCD, 98%), Anhydrous ethanol (99.5%), and 2-methylimidazole (2-MI, 98%) all originated from Aladdin Chemistry Co., Ltd (Shanghai, China). Phytic acid aqueous solution (PA, 70wt%) was purchased by Shanghai Yuanye Bio-Technology Co., Ltd (Shanghai, China). Shanghai Macklin Biochemical Co., Ltd (Shanghai, China) supplied the 1,10-Diaminodecane (DAD, 97%). Anhui Shanfu New Material Technology Co., Ltd (Huangshan, China) supplied solid epoxy resin E12. All reagents were applied with no additional dealing.

Prepared method of PA-DAD

As displayed in Fig. 1a, the PA-DAD was prepared in ethanol-water solution by neutralization reaction. In brief, 18.86 g of PA solution (0.02 mol) and 42.64 g of DAD (0.12 mol) were dissolved into 50 ml of deionized water and 400 ml of anhydrous ethanol, respectively. Then, the PA solution was dropwise added into the stirred DAD solution, yielding in the formation of white precipitate. Subsequently, the final product was acquired by filtration, being washed multiple times by anhydrous ethanol, and dried in a 60 °C vacuum oven for 8 h.

Fabricated method of EP/PA-DAD composites

The different EP/PA-DAD composites were prepared as depicted in the following. The solid epoxy resin E12, along with the prepared PA-DAD, promoter 2-MI and curing agent DCD, were thoroughly mixed using a disintegrator to keep the distribution of mixture uniform. The neutralization reaction occurred at a temperature of 25 °C. The different mixing conditions are displayed in Supplemental Table S1. The above mixture was put in a mold made by stainless steel, and then cured with a press vulcanizer by hot pressing under a pressure of 10 MPa for 25 min at 145 °C. When the temperature was cooled to room temperature, the EP/PA-DAD composites to be used for different tests were obtained.

Characterizations

The characterizations employed in this work mainly include: a nuclear magnetic resonance spectrometer (NMR), Fourier Transform infrared spectroscopy (FTIR), Energy-dispersive X-ray spectroscopy (EDS), Scanning Electron Microscope (SEM), Raman spectra, X-ray photoelectron spectroscopy (XPS), Differential scanning calorimetry (DSC), Thermogravimetry Analysis (TG), Limiting Oxygen Index (LOI), Pyrolysis gas chromatography-mass spectrometry (Py-GC/MS), a cone calorimeter, the tensile strength, the impact strength, and the flexural strength and so on. The corresponding details of characterizations are supplied in the Supporting Information.

Results and discussion

Characterizations of PA-DAD

The FTIR curves of DAD, PA and PA-DAD were carried out as depicted in Fig. 1b. Regarding PA, the 2,400 cm^{-1} peak was

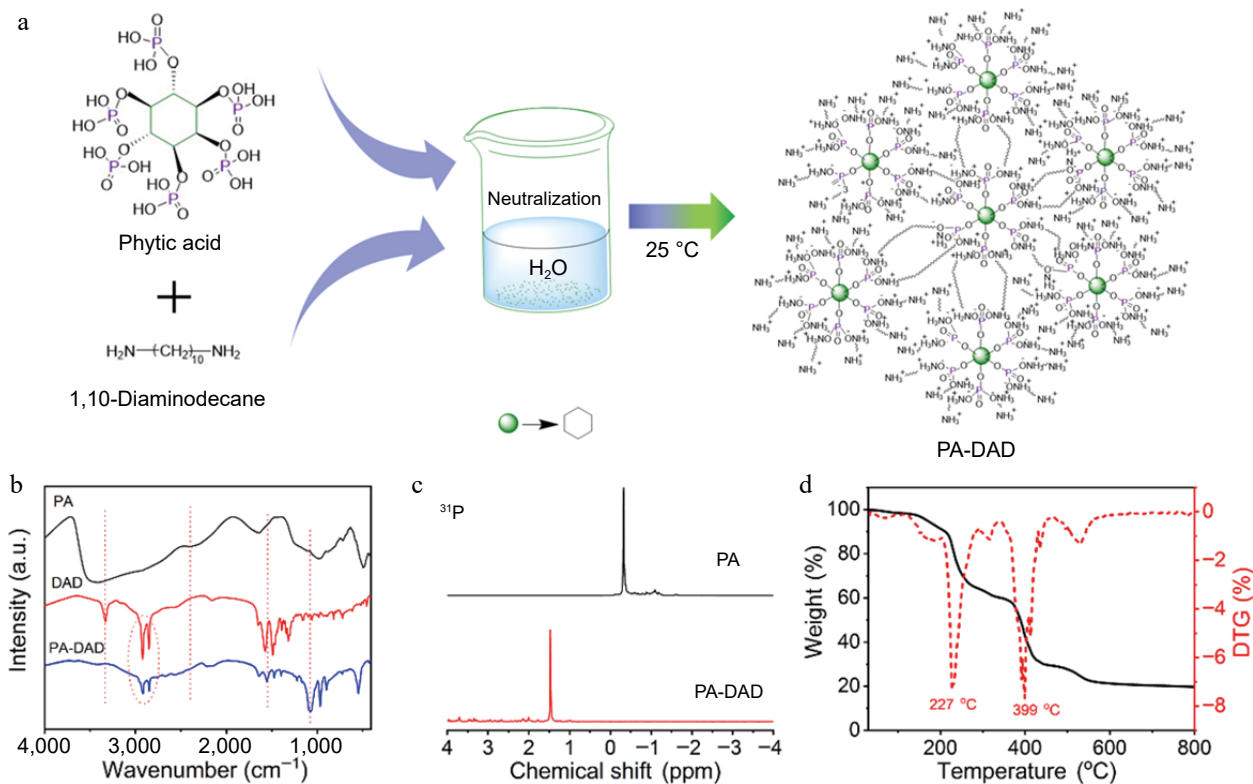


Fig. 1 (a) Schematic diagram for the prepared processing of PA-DAD, (b) FTIR spectra of DAD, PA and PA-DAD, (c) ^{31}P NMR curve of PA-DAD and PA, (d) TG curves of PA-DAD.

Bio-based flame and smoke retardant for epoxy

identified as arising from the (P=O)-OH chemical bond^[34]. In the curve of DAD, the 3,329 cm^{-1} absorption peak corresponded to the stretching vibration of N-H, while the scope for 2,800–3,000 cm^{-1} was related to C-H bonds^[42]. By contrast, the peak assigned to N-H and (P=O)-OH of PA-DAD disappeared. Instead, the new appeared peak of 1,554 cm^{-1} and 1,075 cm^{-1} were ascribed to NH_3^+ and PO_3^{2-} , respectively^[35,43]. The above change suggests that the bio-based ionic complex of PA-DAD was successfully prepared.

Additionally, the chemical structure of PA-DAD was demonstrated *via* ^{31}P NMR, ^1H NMR, and FTIR. As presented in [Supplemental Fig. S1a–S1c](#) and [Fig. 1c](#), the signal peak at 4.8 ppm in all spectra were ascribed to the deuterated water. In the context of PA, two distinct peaks appeared at approximately 4 ppm in the spectrum. Concerning DAD, peaks at 2.5, 1.4, and 1.2 ppm were related to the $-\text{CH}_2-$ protons in various chemical environments. When it comes to PA-DAD, the two peaks at 2.5 and 1.4 ppm exhibited a noticeable shift towards the left, indicating that a neutralization reaction occurred between DAD and PA. Moreover, in the spectra of ^{31}P NMR, as depicted in [Fig. 1b](#), the signal of phosphorus shifted from -0.32 ppm of PA to 1.47 ppm of PA-DAD.

The thermal-degradation behaviors of PA-DAD are also shown in [Fig. 1d](#) and [Supplemental Table 2](#). The process of thermal degradation for PA-DAD involved two primary stages, with the temperatures of maximum weight loss rates recorded at 227 and 399 $^\circ\text{C}$. The initial degradation stage can be attributed to and the dehydration reaction from phytic acid, and the destruction of ionic bonds within PA-DAD^[44]. The second degradation stage was associated with the releasing of NH_3 , H_2O , and also the generated poly-/pyro-/ultra-phosphoric acids as PA-DAD further decomposed^[40,45].

Curing and thermal properties

The curing behaviour from effects of PA-DAD on EP for was explored *via* non isothermal DSC testing. [Supplemental Fig. S2a–S2d](#) displayed the DSC curves of EP/PA-DAD composites with different heating rates of 5, 10, 15, 20, 25 $^\circ\text{C min}^{-1}$ separately. As the heating rate increased, the temperatures of the initial peaks were elevated, and the range of curing temperature became broader because of the intensified thermal effects per unit time^[46]. The reaction activation energy (E_a) had been calculated from Kissinger and Ozawa equation, as shown in [Fig. 2a & b](#) and as well summarized in [Supplemental Table S3](#). The E_a increased significantly when the PA-DAD was incorporated into the EP. The increased presence of active sites, stemming from the amino group of PA-DAD, needed higher energy to be input for chemical reactions during the initial stages of curing. Consequently, compared to pure EP, the EP/PA-DAD systems required higher curing temperatures.

The behaviors of thermal degradation from EP/PA-DAD composites were inspected *via* TG with a nitrogen atmosphere in [Fig. 2c & d](#), and related data were summarized in [Supplemental Table S2](#). The residual mass for EP composites was improved after imparting the PA-DAD. The yields of char for neat EP, EP/10% PA-DAD, EP/20% PA-DAD, and EP/25% PA-DAD composites increased from 11.1% (for neat EP) to 13.6%, 17.1%, and 17.2% at 800 $^\circ\text{C}$, respectively. A higher residual mass indicated an optimistic impact on high flame resistance of composites. Compared with neat EP, the T_{onset} (the temperature at 5 wt% mass loss) and T_{max} (the maximum degradation temperature) of EP/PA-DAD decreased continuously as the increased addition amount of PA-DAD. The initial thermal decomposition of EP/PA-DAD primarily resulted from the premature breakdown of PA-DAD. Consequently, PA-DAD can be decomposed as poly-/pyro-/ultra-phosphoric acids at lower temperatures,

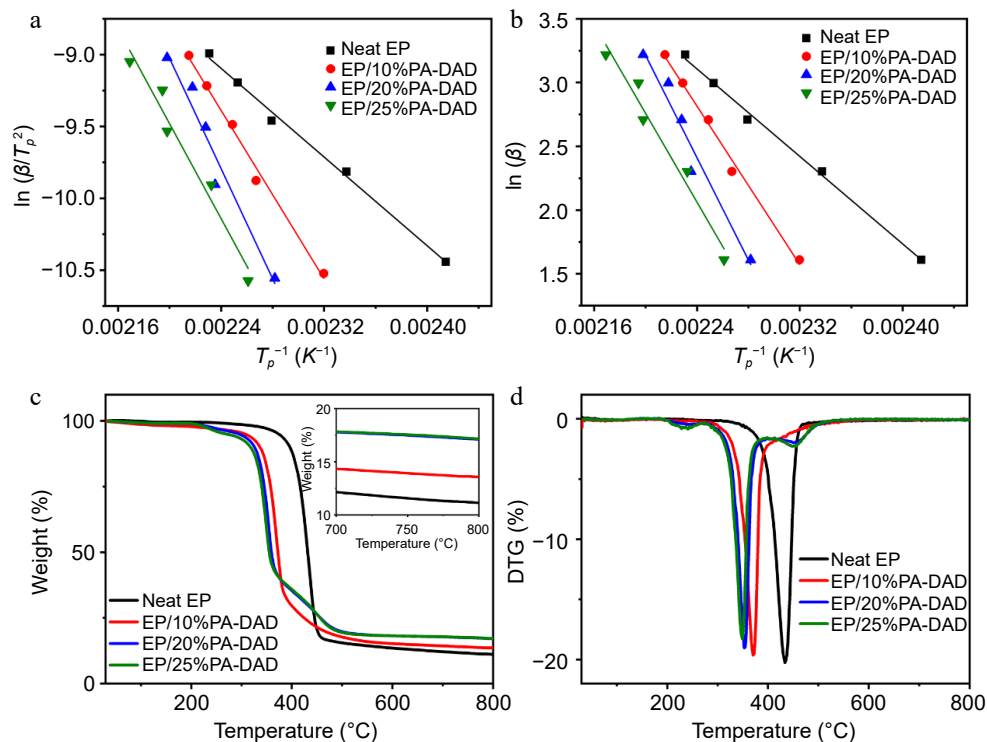


Fig. 2 The calculated results of (a) Kissinger, and (b) Ozawa methods for neat EP and its different composites, (c) TG and (d) DTG curves for EP composites.

accelerating the decomposition of EP matrix. The generated poly-/pyro-/ultra-phosphoric acids facilitated crosslinking reactions and catalyzed the carbonization of EP molecules. The process could lead to the formatting for a protective and stable char layer during high-temperature stages. The protective layer significantly enhanced the fire retardancy for EP composites during combustion, providing a safeguard for the underlying matrix^[47,48].

Flame retardancy for EP composites

Both LOI values as well as the UL-94 rating were initially employed to assess the flame retardancy for EP composites, and corresponding data and results are summarized in Table 1. Neat EP, which is inherently flammable, exhibited a quite low LOI value of 20.4% and did not meet V-0 rating in the test of UL-94. Upon adding PA-DAD into EP, there were significant increases in LOI values of EP composites. When the content of PA-DAD reached 25 wt%, a notably high LOI value with 28.0%

Table 1. Detailed results corresponding to UL-94 and LOI for EP composites.

Sample	UL-94			LOI (%)
	Rating	Dripping	t ₁ /t ₂ (s)	
Neat EP	NR	YES	>30	20.4
EP/10%PA-DAD	NR	NO	>30	23.6
EP/20%PA-DAD	V-1	NO	8.0/2.4	25.3
EP/25%PA-DAD	V-0	NO	1.1/0.9	28.0

for the EP/25% PA-DAD composite was achieved and successfully satisfied V-0 rating in the test of UL-94 (as indicated in Supplemental Fig. S3). The above findings demonstrated that PA-DAD served as an efficient biological flame retardant for EP, enhancing fire resistance of composites.

Cone calorimetry tests were performed to assess the actual fire performance for EP composites, and the associated results are reviewed in Table 2. EP/PA-DAD composites' time to ignition (TTI) was found to be shorter than that for pure EP. Because an earlier decomposition for PA-DAD would form a stable, and protective char layer, keeping the EP matrix from further thermal degradation. As depicted in Fig. 3a, the highly flammable EP would burn out rapidly after ignition, and its peak heat release rate (pHRR) was 1,007 kW/m². Reversely, after introducing 25 wt% PA-DAD to EP, the pHRR of the composites has been reduced to 280 kW/m², decreasing by 72.2% than that of neat EP. Moreover, as shown in Supplemental Fig. S4, the total heat release (THR) reduced significantly from 99.2 MJ/m² of pure EP to 71.2 MJ/m² of EP/25% PA-DAD, which had decreased by 28.3%. Besides, the rate of fire growth (FIGRA) was the ratio between pHRR and T_{pHRR} (time to pHRR) according to the HRR curves to evaluate the actual fire hazard for material qualitatively^[49,50]. The FIGRA value (1.38 kW/m²·s) of EP/25% PA-DAD was 77.8% lower than that of neat EP with 6.21 kW/m²·s, underscoring the superior fire safety enhancement achieved by PA-DAD in the EP composites. Additionally, the smoke released during combustion was generally recognized as another critical factor in evaluating the fire retardancy of the material. In

Table 2. Data from Cone calorimeter for EP and its composites.

Samples	TTI (s)	T _{pHRR} (s)	pHRR (kW/m ²)	THR (MJ/m ²)	pSPR (m ² /s)	TSP (m ²)	pCOP (g/s)	pCO ₂ P (g/s)	FIGRA (kW/m ² ·s)
Neat EP	86 ± 3	162 ± 5	1007 ± 32	99.2 ± 1.9	0.26 ± 0.010	27.7 ± 2.1	0.0258 ± 0.0007	0.586 ± 0.013	6.21
EP/10% PA-DAD	71 ± 2	121 ± 4	740 ± 26	96.1 ± 2.1	0.28 ± 0.012	25.1 ± 1.7	0.0274 ± 0.0006	0.343 ± 0.009	6.12
EP/20% PA-DAD	63 ± 2	184 ± 4	403 ± 24	71.9 ± 0.7	0.12 ± 0.006	16.6 ± 0.9	0.0125 ± 0.0005	0.176 ± 0.007	2.19
EP/25% PA-DAD	34 ± 1	203 ± 3	280 ± 19	71.2 ± 0.9	0.11 ± 0.007	14.0 ± 1.1	0.0086 ± 0.0003	0.124 ± 0.008	1.38

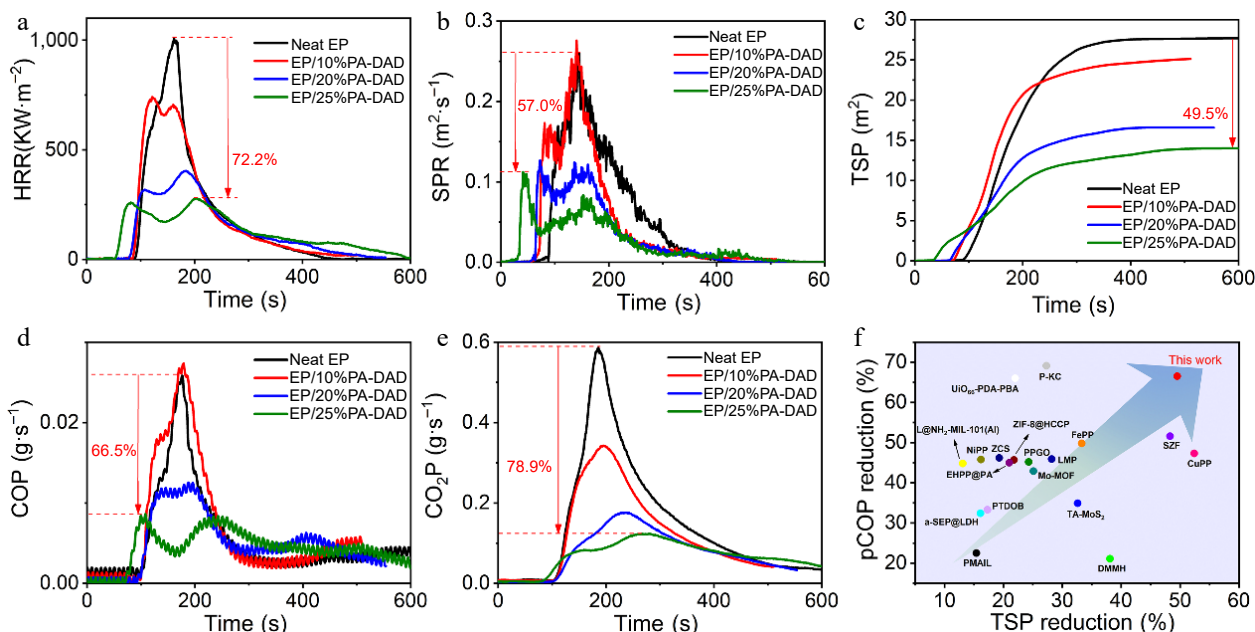


Fig. 3 (a) HRR, (b) SPR, (c) TSP, (d) COP, (e) CO₂P curves vs time for EP composites under a flux with 35 kW/m², and (f) the TSP reduction vs pCOP reduction of PA-DAD compared with other works.

Bio-based flame and smoke retardant for epoxy

Fig. 3b & c, the total smoke product (TSP) and peak of smoke product rate (pSPR) values of EP/PA-DAD composites were inhibited significantly. The values of THR and pHRR for the EP/25% PA-DAD composite experienced noteworthy reductions of 49.5% and 57.0%, respectively, in contrast with neat EP. In detail, as presented in Fig. 3d & e, the peak of CO production named pCOP, and the peak of CO₂ production named pCO₂P for EP/25% PA-DAD decreased by 66.5%, and 78.9%, respectively. In the event of a fire, fatalities can occur due to suffocation when the concentrations of carbon dioxide (CO₂), and carbon monoxide (CO) in the surrounding air reach critical levels. Thus, the introduced PA-DAD to EP dramatically improved the fire safety and provided more escaped time for people. Moreover, lower production of CO and CO₂ disclosed the more carbon fixed char residue during combustion, contributing to exert condensed phase effect for flame-retardant mechanism. To underscore the superior attributes of the

newly formulated PA-DAD, the TSP reduction, pCOP reduction of PA-DAD and previously reported flame retardant for EP are displayed in Fig. 3f. The detailed fire performances are also summarized as in Supplemental Table S4. The biological PA-DAD in this work showed a significant reduction of TSP and pCOP than those of previous reported FRs.

Flame-retardant mechanism

To disclose the mechanisms from flame retardants within EP matrix, the char residues of EP composites from cone calorimetry were further studied. As displayed in Fig. 4, the digital photos indicated that EP/PA-DAD composites had a dense and intumescent carbon layer. With an increasing loading of PA-DAD, the volumes of residues increased as well expanded gradually. The dense and intumescent carbon layer provided a desired shield to reduce the heat and mass transferring between condensed and gas phases. SEM-EDS was applied to

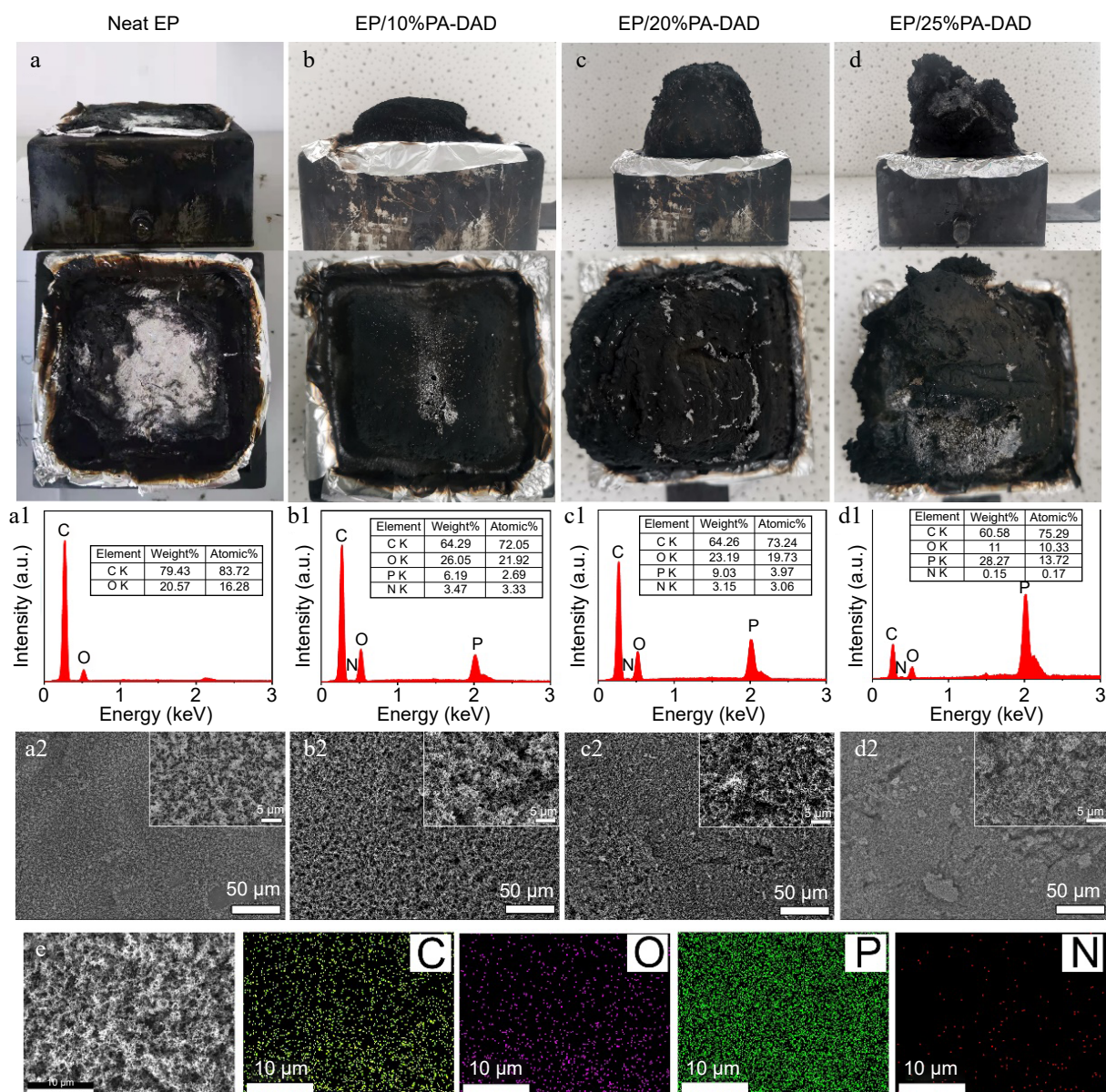


Fig. 4 Digital photos of residual chars from cone calorimetry for (a) neat EP, (b) EP/10% PA-DAD, (c) EP/20% PA-DAD, (d) EP/25% PA-DAD. (a1)–(d1) EDS results and (a2)–(d2) SEM photos for corresponding residue char. (e) The images of elemental mapping for residue chars of EP/25% PA-DAD.

evaluate the quality of char residues. As depicted in Fig. 4a1–d1 & 4e, there were four elements including C, O, N and P in the char residues of EP/PA-DAD composites. And P content of the char layer was increased gradually with the increased loading of PA-DAD. The element P was introduced by PA-DAD, accelerating the catalysis and carbonization for EP to produce a good char layer in dense, continuous, and phosphorous-containing. Thus, the char layers of EP/PA-DAD composites in Fig. 4a2–d2 were relatively compact compared with neat EP, enhancing the flame retardancy *via* condensed phase.

The compositions of char residues were also analyzed by FTIR methods. In Supplemental Fig. S5a, the absorption peaks at around 1,618, and 2,852–2,958 cm^{-1} were related to C=C, and C-H' stretching vibration from CH_2 group, respectively^[33,43]. For EP/25% PA-DAD, a new 1,160 cm^{-1} absorption peak indicated the presence of P-O bonds in compound. Two typical peaks of G band at 1,580 cm^{-1} and D band at 1,350 cm^{-1} were presented in Raman spectra of char residues for EP and EP/25% PA-DAD composite, which corresponded to graphite char and the disordered char, respectively (see Supplemental Fig. S5b)^[51]. The value of I_D/I_G for EP/25% PA-DAD char was 1.11, higher than that of char from neat EP (0.89), suggesting a

smaller microstructure size that enhances fire resistance^[52]. As displayed in Supplemental Fig. S5c, the composition of elements from the surface of EP/25% PA-DAD char was analyzed by XPS. The elements including C, N, O, and P existed in the chemical structure of EP/25% PA-DAD char, which was consistent with the results of EDS characterization. The high-resolution of elements was shown in Supplemental Fig. S6a–S6d. Three peaks of C-C in aliphatic and aromatic species at 284.5 eV, C=O at 288.5 eV, and C-O in ether and/or hydroxyl group at 286.0 eV were deconvoluted from C1s spectra. In the high-resolution O1s, three kinds of oxygen configurations appear at 535.1, 532.1 and 530.4 eV, corresponding to -COOH, -O- of C-O-C or C-O-P and =O from phosphate or carbonyl groups, respectively. The N1s spectra could be divided into two peaks of 400.2 and 399.2 eV, assigning to nitrogen functionality in the pyrrolic group and oxidized nitrogen compounds^[53,54]. The only 133.5 eV peak from P2p spectra was ascribed to pyrophosphate and polyphosphate. The results of XPS demonstrated that poly-/pyro-/ultra-phosphoric acids were generated while the combustion occurred, forming a strong char layer *via* dehydration and esterification of EP.

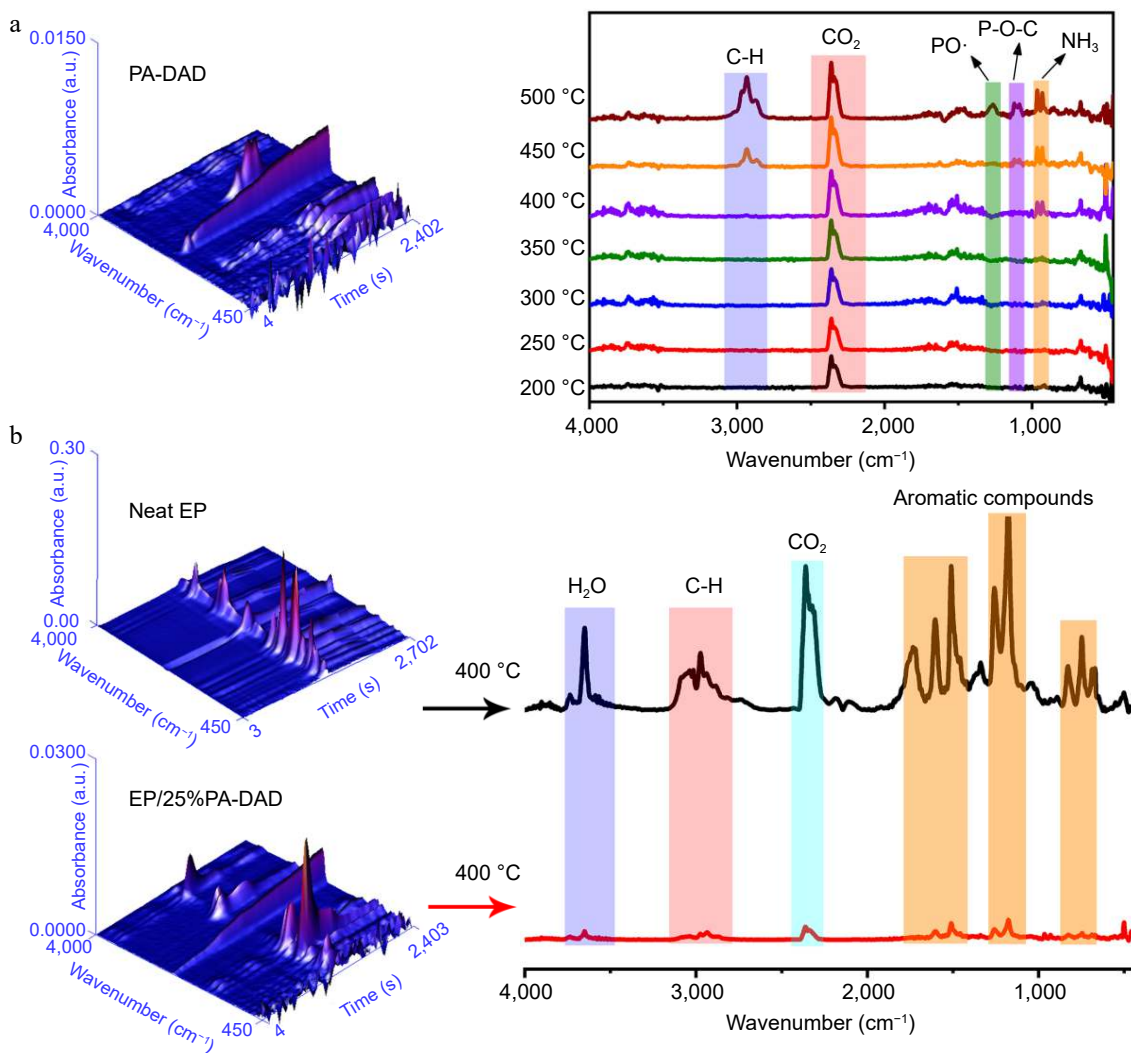


Fig. 5 (a) FTIR 3D and 2D spectra from pyrolysis products for PA-DAD. (b) FTIR 3D and 2D spectra from the pyrolysis products for pure EP and EP/25% PA-DAD with the maximum rate of decomposition.

Bio-based flame and smoke retardant for epoxy

The TG-IR was carried out to explore the pyrolysis products of PA-DAD, pure EP and EP/25%PA-DAD composite under a heating rate with 20 °C/min and N₂ atmosphere. Figure 5a showed the FTIR 3D and 2D for decomposed fragments from PA-DAD at 200–500 °C when thermal degradation. The primary gaseous products of PA-DAD were hydrocarbons at 2970 cm⁻¹, CO₂ at 2360 cm⁻¹, PO· at 1258 cm⁻¹, P-O-C at 1097 cm⁻¹ and NH₃ at both 965 and 930 cm⁻¹. The fragments with P-O-C and PO· were demonstrated by a strong signal at 450–500 °C, being capable of quenching active radicals with OH· and H· during burning, thereby suppressing the combustion. The absorption peak for NH₃ was displayed between 400–500 °C, which contributed to the dilution of flue gases and a reduction in the rate of burning. In Fig. 5b, both neat EP and EP/25% PA-DAD displayed the analogous characteristic peaks from gaseous products when degradation, such as aromatic compounds at 1,605, 1,510, 834 and 689 cm⁻¹, hydrocarbons at 2,800–3,000 cm⁻¹, CO₂ at 2,360 cm⁻¹, H₂O at 3,600–4,000 cm⁻¹.

Nevertheless, the EP/25% PA-DAD showed the weaker peak intensities compared with pure EP, indicating the incorporation for PA-DAD could obstacle some productions of volatiles effectively during burning. In addition, the curves of total volatile gas intensity versus temperatures, and the Gram-Schmidt (GS) curves for pure EP and EP/25% PA-DAD composite are depicted in Supplemental Fig. S7. The EP/25% PA-DAD composite's intensities of pyrolytic products were lower than that of neat EP consistently. Some reasons for the dramatical reduction of volatile pyrolysis products from EP/25% PA-DAD are as follows. At the beginning of combustion, the earlier thermal decomposition for PA-DAD could lead to the carbonization layers with nano-scale, acting as a block to inhibit the transferring of heat and mass. When combustion continues, the PA-DAD generated poly-/pyro-/ultra-phosphoric acids for catalyzing the degradation of EP, forming intumescent and compact char for protecting the matrix from further thermal degradation.

Pyrolysis behaviors

The pyrolysis products obtained from EP/PA-DAD composites were investigated by the method of Py-GC/MS further. The main pyrolysis products from the pyrogram (in Supplemental Fig. S8) for EP/25% PA-DAD, were also listed in Supplemental Table S5. The 2, 3, 5, 6, and 10 peaks in the pyrogram were attributed to phenol, p-Cresol, 4-isopropyl phenol, 4-isopropenylphenol, and 2,2-bis(4-hydroxyphenyl) propane. The aforementioned substances stemmed from the reactions involving the opening of aromatic rings and the subsequent rearrangement reactions of the bisphenol A chains. The nitrogen-containing compounds of (E)-Alpha-cyanocinnamamide at peak 8, have the capacity to decompose into non-flammable, small-molecule gas NH₃. Above decomposition process effectively reduced the concentration of the flammable gases^[55]. The detailed pyrolysis routes and speculative flame-retardant mechanism for EP/25% PA-DAD are shown in Fig. 6. During the burning process, the decomposition of PA-DAD can yield products with P-O-C, PO·, and NH₃, thereby capturing the active radicals of H·, OH· and decreasing the flammable gases. When combustion continues, the residual phosphorus from condensed generated the poly-/pyro-/ultra-phosphoric acids, catalyzing the degradation of EP for promoting the producing of the intumescent and compact chars. Herein, the formation of intumescent and compact chars reduced the oxygen, and toxic

gas emissions to prevent the matrix from continuously degrading. Thus, the above results about incorporated PA-DAD further demonstrate the excellent flame retardancy and enhanced residual char of composites.

Mechanical properties

Mechanical performances including the tensile, flexural and impact strength for neat EP as well EP/PA-DAD composites are displayed in Figs. 7 & 8. The above relatively detailed data are reviewed in Supplemental Table S6. In Fig. 7a & d, the typical strain-stress for neat EP and its corresponding composites are presented. As demonstrated in Fig. 7c & f, the toughness values of pure EP and its corresponding composites were calculated by the integration values from stress-strain curves^[56,57]. Obviously, the tensile, flexural strength and toughness were firstly increased and then decreased with the increasing contents of PA-DAD. Partial increased modulus can be attributed to the capacity of PA-DAD to enhance crosslink density. The increased toughness was assigned to the ion bonds formed by PA-DAD, which have the effect on dissipating energy^[12,58]. The partial agglomeration of PA-DAD will be caused after the added amount reaches a certain level, leading to a noticeable decline in mechanical properties of EP composites^[44].

The PA-DAD were agglomerated in the EP matrix as seen in the tensile fracture when the addition reached 25 wt% (see Fig. 8). The mapping photograph also proved the phosphorus agglomeration in the fracture. When the PA-DAD loading was 10 wt%, the tensile, and flexural strength of composites owned higher values compared with neat EP, which were 17.8% and 26.0% respectively. In particular, the tensile, and flexural toughness were greatly enhanced by 466% and 178% compared with neat EP. When PA-DAD loading reached 20 wt% and 25 wt%, although the tensile, and flexural strength of EP/PA-DAD composites exhibited lower values, the tensile, and flexural toughness still higher than those of neat EP. Some agglomerations caused by the relatively high filler contents led to the tensile and flexural strength decreased, but the ion bonds formed by PA-DAD have the function of dissipating energy for increasing tensile and flexural toughness. In comparison with neat EP, the impact strength (Supplemental Table S6) of EP/10% PA-DAD, EP/20% PA-DAD, and EP/25% PA-DAD were enhanced to 14.61, 13.00 and 8.53 KJ·m⁻², and were also enhanced by 99.0%, 77.1%, and 16.2%, respectively.

Conclusions

In conclusion, a fully biological flame retardant named PA-DAD has been successfully prepared through a straightforward neutralization reaction of DAD and PA. When the content of PA-DAD achieved 25 wt%, LOI value for EP/25% PA-DAD composite reached up to 28.0%, and also satisfied a V-0 rating of the UL-94 test. In comparison with neat EP, the EP/25% PA-DAD displayed dramatic reductions in pHRR (72.2%), pSPR (57.0%), THR (28.3%), TSP (49.5%) and FIGRA (77.8%). The imparting of PA-DAD can also inhibit the production of volatiles sufficiently. The synergy between condensed and gas phase contributed to the outstanding flame retardancy from EP/PA-DAD composites, beneficial to proposed flame retardant mechanisms. For the condensed phases, PA-DAD generated poly-/pyro-/ultra-phosphoric acids and facilitated the production of a protective char shield to insulate the transferring of heat and mass. While in the gas phases, the PA-DAD released the PO·, P-O-C, and NH₃ and then quenched the active

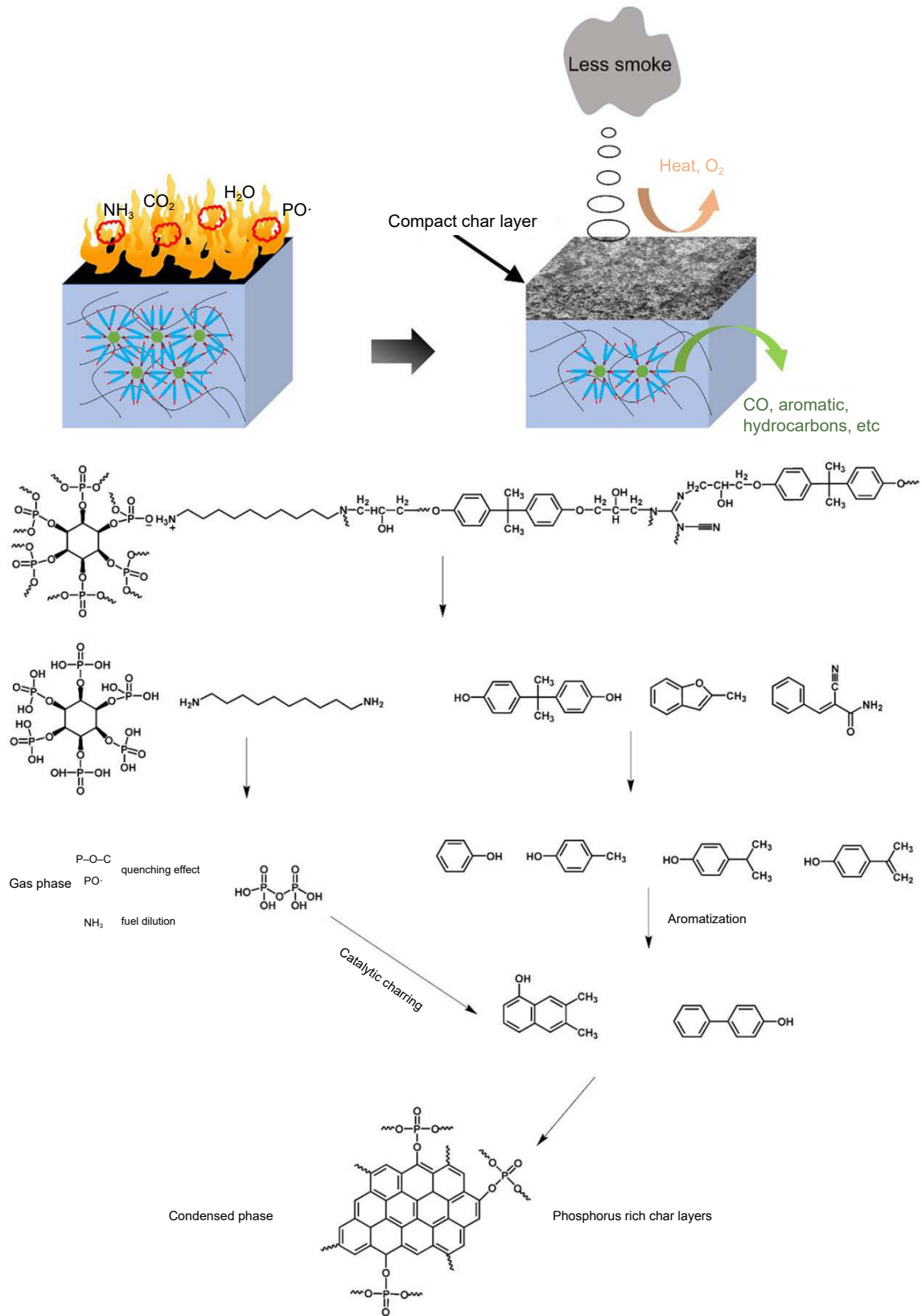


Fig. 6 Speculated pyrolysis and flame-retardant mechanisms for composites with PA-DAD.

radicals of H· and OH·. The mechanical performances for EP composites have been enhanced to certain degrees after adding the flame retardant of PA-DAD. Our work supplied a

friendly and facile approach for preparing biological flame retardant and smoke suppressant materials for high fire-safety required EP composites.

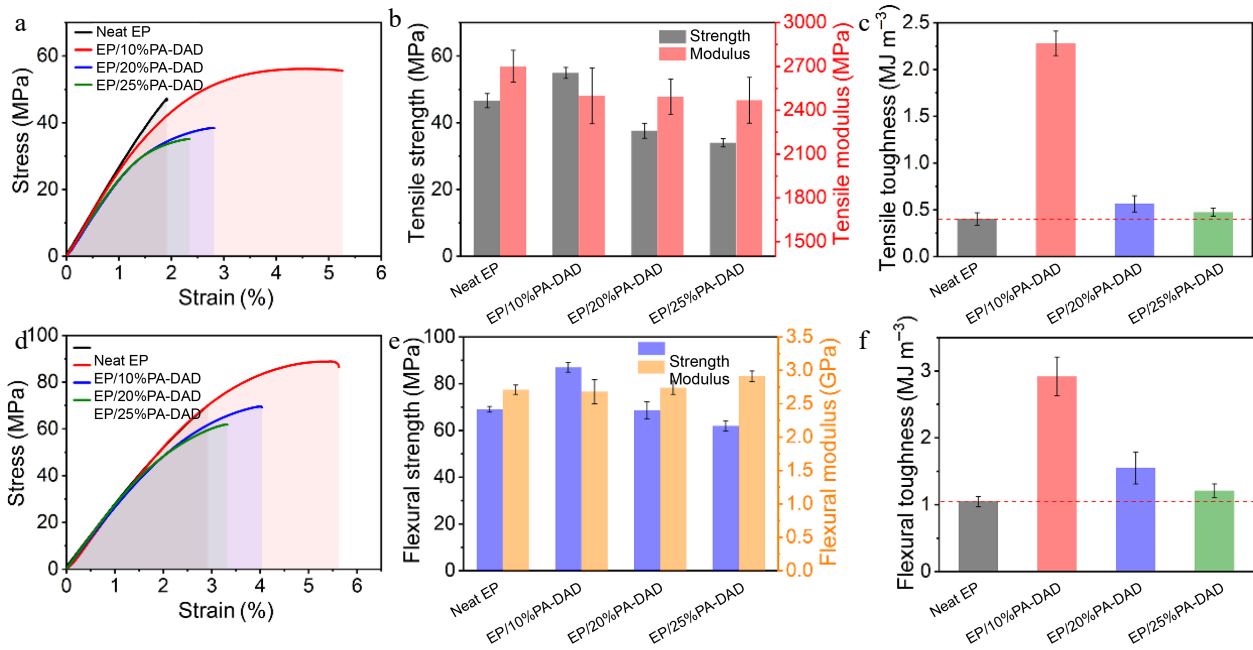


Fig. 7 (a) Tensile stress-strain curves, (b) tensile strength and modulus, (c) tensile toughness, (d) flexural stress-strain curves (e) flexural strength, (f) flexural toughness for EP and its corresponding composites.

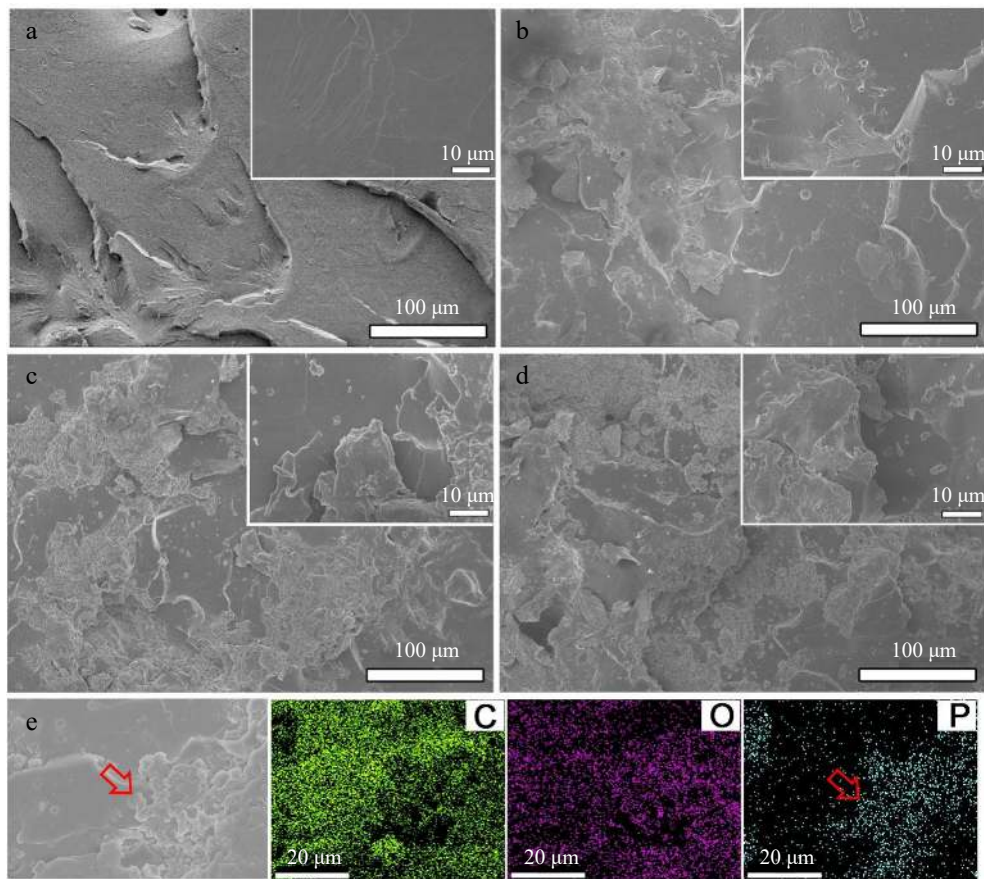


Fig. 8 SEM images from the fractured surfaces of tensile samples for (a) neat EP, (b) EP/10% PA-DAD, (c) EP/20% PA-DAD, and (d) EP/25% PA-DAD. (e) EDS mapping photograph of tensile fractured surfaces for EP/25% PA-DAD.

Author contributions

The authors confirm contribution to the paper as follows: study conception and design: Lin Z, Zhang W, Dai J; data collection: Lin Z, Zhang W, Lou G, Bai Z; analysis and interpretation of results: Lou G, Bai Z, Xu J, Li H, Zong Y, Chen F, Song P, Liu L, Dai J; draft manuscript preparation: Lin Z, Lou G, Chen F, Dai J. All authors reviewed the results and approved the final version of the manuscript.

Data availability

The datasets generated and analyzed during the current study are available from the corresponding author on reasonable request.

Acknowledgments

This work was financially supported by the National Natural Science Foundation of Zhejiang Province (No. LY21E030001), National Natural Science Foundation of China (No. 51903222), National College Students Innovation and Entrepreneurship Training Program of China (No. 202210341055), the 'Leading geese' projects of Zhejiang Provincial Department of Science and Technology (No. 2022C03128), and the College Student Science and Technology Innovation Activity Plan of Zhejiang Province (No. 2023R412019).

Conflict of interest

The authors declare that they have no conflict of interest.

Supplementary Information accompanies this paper at (<https://www.maxapress.com/article/doi/10.48130/EMSt-2023-0021>)

Dates

Received 17 October 2023; Accepted 12 December 2023; Published online 26 December 2023

References

1. Kong Q, Wu T, Zhang J, Wang DY. 2018. Simultaneously improving flame retardancy and dynamic mechanical properties of epoxy resin nanocomposites through layered copper phenylphosphate. *Composites Science and Technology* 154:136–44
2. Gholipour-Mahmoudalilou M, Roghani-Mamaqani H, Azimi R, Abdollahi A. 2018. Preparation of hyperbranched poly (amidoamine)-grafted graphene nanolayers as a composite and curing agent for epoxy resin. *Applied Surface Science* 428:1061–69
3. Fang F, Song P, Ran S, Guo Z, Wang H, et al. 2018. A facile way to prepare phosphorus-nitrogen-functionalized graphene oxide for enhancing the flame retardancy of epoxy resin. *Composites Communications* 10:97–102
4. Xu B, Zhang Q, Zhou H, Qian L, Zhao S. 2023. Small change, big impact: Simply changing the substitute on Si atom towards significant improvement of flame retardancy and toughness of epoxy resins. *Composites Part B: Engineering* 263:110832
5. Xu B, Wei S, Liu Y, Wu M. 2023. Effects of different metal ions in phosphonitrile-modified organometallic complexes on flame retardancy of epoxy resin. *Polymer Degradation and Stability* 214:110407
6. Li D, Zhang Z, Wang S, Xu M, Li B. 2022. A monomolecular intumescent flame retardant for improvement simultaneously of fire safety, smoke suppression, and mechanical properties of epoxy resin. *Journal of Applied Polymer Science* 139:52104
7. Luo F, Wu K, Wang S, Lu M. 2017. Melamine resin/graphite nanoflakes hybrids and its vacuum-assisted prepared epoxy composites with anisotropic thermal conductivity and improved flame retardancy. *Composites Science and Technology* 144:100–6
8. Huo S, Yang S, Wang J, Cheng J, Zhang Q, et al. 2020. A liquid phosphorus-containing imidazole derivative as flame-retardant curing agent for epoxy resin with enhanced thermal latency, mechanical, and flame-retardant performances. *Journal of Hazardous Materials* 386:121984
9. Huo S, Yang S, Wang J, Cheng J, Zhang Q, et al. 2020. A Liquid Phosphaphenanthrene-Derived Imidazole for Improved Flame Retardancy and Smoke Suppression of Epoxy Resin. *ACS Applied Polymer Materials* 2:3566–75
10. Xu B, Wu M, Liu Y, Wei S. 2023. Study on flame retardancy behavior of epoxy resin with phosphaphenanthrene triazine compound and organic zinc complexes based on phosphonitrile. *Molecules* 28:3069
11. Xu B, Wei S, Liu Y, Zhao S, Qian L. 2022. Preparation of an organometallic complex based on phosphonitrile and its flame retardant application in epoxy resin. *Journal of Materials Research and Technology* 21:4921–39
12. Lou G, Rao Q, Li Q, Bai Z, He X, et al. 2023. Novel ionic complex with flame retardancy and ultrastrong toughening effect on epoxy resin. *Chemical Engineering Journal* 455:139334
13. Xu B, Liu Y, Wei S, Zhao S, Qian L, et al. 2022. A Phosphorous-Based Bi-Functional Flame Retardant Based on Phosphaphenanthrene and Aluminum Hypophosphite for an Epoxy Thermoset. *International Journal of Molecular Sciences* 23:11256
14. Ma W, Xu B, Shao L, Liu Y, Chen Y, et al. 2019. Synthesis of (1,4-Methylenephénylphosphinic acid) Piperazine and Its Application as a Flame Retardant in Epoxy Thermosets. *Macromolecular Materials and Engineering* 304:1900419
15. Huo S, Song P, Yu B, Ran S, Chevali VS, et al. 2021. Phosphorus-containing flame retardant epoxy thermosets: Recent advances and future perspectives. *Progress in Polymer Science* 114:101366
16. He W, Song P, Yu B, Fang Z, Wang H. 2020. Flame retardant polymeric nanocomposites through the combination of nanomaterials and conventional flame retardants. *Progress in Materials Science* 114:100687
17. Xue Y, Shen M, Zeng S, Zhang W, Hao L, et al. 2019. A novel strategy for enhancing the flame resistance, dynamic mechanical and the thermal degradation properties of epoxy nanocomposites. *Materials Research Express* 6(12):125003
18. Huang G, Chen W, Wu T, Guo H, Fu C, et al. 2021. Multifunctional graphene-based nano-additives toward high-performance polymer nanocomposites with enhanced mechanical, thermal, flame retardancy and smoke suppressive properties. *Chemical Engineering Journal* 410:127590
19. Xue Y, Feng J, Huo S, Song P, Yu B, et al. 2020. Polyphosphoramidate-intercalated MXene for simultaneously enhancing thermal stability, flame retardancy and mechanical properties of poly(lactide). *Chemical Engineering Journal* 397:125336
20. Zhang Y, Jing J, Liu T, Xi L, Sai T, et al. 2021. A molecularly engineered bioderived polyphosphate for enhanced flame retardant, UV-blocking and mechanical properties of poly(lactic acid). *Chemical Engineering Journal* 411:128493
21. Xu Y, Liu L, Yan C, Hong Y, Xu M, et al. 2021. Eco-friendly phosphonic acid piperazine salt toward high-efficiency smoke suppression and flame retardancy for epoxy resins. *Journal of Materials Science* 56:16999–7010
22. Feng J, Sun Y, Song P, Lei W, Wu Q, et al. 2017. Fire-resistant, strong, and green polymer nanocomposites based on poly(lactic acid) and core-shell nanofibrous flame retardants. *ACS Sustainable Chemistry & Engineering* 5:7894–904
23. Yin W, Chen L, Lu F, Song P, Dai J, et al. 2018. Mechanically robust, flame-retardant poly(lactic acid) biocomposites via combining cellulose nanofibers and ammonium polyphosphate. *ACS Omega* 3:5615–26

Bio-based flame and smoke retardant for epoxy

24. Yang H, Shi B, Xue Y, Ma Z, Liu L, et al. 2021. Molecularly engineered lignin-derived additives enable fire-retardant, UV-shielding, and mechanically strong polylactide biocomposites. *Biomacromolecules* 22:1432–44
25. Liu L, Qian M, Song Pa, Huang G, Yu Y, et al. 2016. Fabrication of green lignin-based flame retardants for enhancing the thermal and fire retardancy properties of polypropylene/wood composites. *ACS Sustainable Chemistry & Engineering* 4:2422–31
26. Liu L, Huang G, Song P, Yu Y, Fu S. 2016. Converting industrial alkali lignin to biobased functional additives for improving fire behavior and smoke suppression of polybutylene succinate. *ACS Sustainable Chemistry & Engineering* 4:4732–42
27. Yang H, Yu B, Xu X, Bourbigot S, Wang H, et al. 2020. Lignin-derived bio-based flame retardants toward high-performance sustainable polymeric materials. *Green Chemistry* 22:2129–61
28. Lou G, Ma Z, Dai J, Bai Z, Fu S, et al. 2021. Fully biobased surface-functionalized microcrystalline cellulose via green self-assembly toward fire-retardant, strong, and tough epoxy biocomposites. *ACS Sustainable Chemistry & Engineering* 9:13595–605
29. Mendis GP, Weiss SG, Korey M, Boardman CR, Dietenberger M, et al. 2016. Phosphorylated lignin as a halogen-free flame retardant additive for epoxy composites. *Green Materials* 4:150–59
30. Guo W, Wang X, Gangireddy CSR, Wang J, Pan Y, et al. 2019. Cardanol derived benzoxazine in combination with boron-doped graphene toward simultaneously improved toughening and flame retardant epoxy composites. *Composites Part A: Applied Science and Manufacturing* 116:13–23
31. Wang X, Zhou S, Guo WW, Wang PL, Xing W, et al. 2017. Renewable cardanol-based phosphate as a flame retardant toughening agent for epoxy resins. *ACS Sustainable Chemistry & Engineering* 5:3409–16
32. Li C, Wan J, Kalali EN, Fan H, Wang DY. 2015. Synthesis and characterization of functional eugenol derivative based layered double hydroxide and its use as a nanoflame-retardant in epoxy resin. *Journal of Materials Chemistry A* 3:3471–79
33. Fang F, Huo S, Shen H, Ran S, Wang H, et al. 2020. A bio-based ionic complex with different oxidation states of phosphorus for reducing flammability and smoke release of epoxy resins. *Composites Communications* 17:104–8
34. Zhu ZM, Shang K, Wang LX, Wang JS. 2019. Synthesis of an effective bio-based flame-retardant curing agent and its application in epoxy resin: Curing behavior, thermal stability and flame retardancy. *Polymer Degradation and Stability* 167:179–88
35. Wang P, Liao D, Hu X, Pan N, Li W, et al. 2019. Facile fabrication of biobased P–N–C-containing nano-layered hybrid: Preparation, growth mechanism and its efficient fire retardancy in epoxy. *Polymer Degradation and Stability* 159:153–62
36. Zhang J, Mi X, Chen S, Xu Z, Zhang D, et al. 2020. A bio-based hyperbranched flame retardant for epoxy resins. *Chemical Engineering Journal* 381:122719
37. Yang D, Dong L, Hou X, Zheng W, Xiao J, et al. 2020. Synthesis of bio-based poly (cyclotriphosphazene-resveratrol) microspheres acting as both flame retardant and reinforcing agent to epoxy resin. *Polymers for Advanced Technologies* 31:135–45
38. Li Z, Liu Z, Zhang J, Fu C, Wagenknecht U, et al. 2019. Bio-based layered double hydroxide nanocarrier toward fire-retardant epoxy resin with efficiently improved smoke suppression. *Chemical Engineering Journal* 378:122046
39. Zhao X, Xiao D, Alonso JP, Wang DY. 2017. Inclusion complex between beta-cyclodextrin and phenylphosphonicdiamide as novel bio-based flame retardant to epoxy: Inclusion behavior, characterization and flammability. *Materials & Design* 114:623–32
40. Gao YY, Deng C, Du YY, Huang SC, Wang YZ. 2019. A novel bio-based flame retardant for polypropylene from phytic acid. *Polymer Degradation and Stability* 161:298–308
41. Wang D, Wang Y, Li T, Zhang S, Ma P, et al. 2020. A bio-based flame-retardant starch based on phytic acid. *ACS Sustainable Chemistry & Engineering* 8:10265–74
42. Wang WZ, Zhang YH. 2010. Synthesis of semiaromatic polyamides based on decanediamine. *Chinese Journal of Polymer Science* 28:467–73
43. Zhang T, Yan H, Shen L, Fang Z, Zhang X, et al. 2014. A phosphorus-, nitrogen- and carbon-containing polyelectrolyte complex: preparation, characterization and its flame retardant performance on polypropylene. *RSC Advances* 4:48285–92
44. Zhu ZM, Xu YJ, Liao W, Xu S, Wang YZ. 2017. Highly flame retardant expanded polystyrene foams from Phosphorus–Nitrogen–Silicon synergistic adhesives. *Industrial & Engineering Chemistry Research* 56:4649–58
45. Tan Y, Shao ZB, Yu LX, Long JW, Qi M, et al. 2016. Piperazine-modified ammonium polyphosphate as monocomponent flame-retardant hardener for epoxy resin: flame retardance, curing behavior and mechanical property. *Polymer Chemistry* 7:3003–12
46. Ali Lakho D, Yao D, Cho K, Ishaq M, Wang Y. 2017. Study of the curing kinetics toward development of fast-curing epoxy resins. *Polymer-Plastics Technology and Engineering* 56:161–70
47. Laufer G, Kirkland C, Morgan AB, Grunlan JC. 2012. Intumescent multilayer nanocoating, made with renewable polyelectrolytes, for flame-retardant cotton. *Biomacromolecules* 13:2843–48
48. Gao M, Wu W, Yan Y. 2009. Thermal degradation and flame retardancy of epoxy resins containing intumescent flame retardant. *Journal of Thermal Analysis and Calorimetry* 95:605–4
49. Yan YW, Chen L, Jian RK, Kong S, Wang YZ. 2012. Intumescence: An effect way to flame retardance and smoke suppression for polystyrene. *Polymer Degradation and Stability* 97:1423–31
50. Breulet H, Steenhuizen T. 2005. Fire testing of cables: comparison of SBI with FIPEC/Europacable tests. *Polymer Degradation and Stability* 88:150–58
51. Xing W, Zhang P, Song L, Wang X, Hu Y. 2014. Effects of alpha-zirconium phosphate on thermal degradation and flame retardancy of transparent intumescent fire protective coating. *Materials Research Bulletin* 49:1–6
52. Yang G, Wu WH, Wang YH, Jiao YH, Lu LY, et al. 2019. Synthesis of a novel phosphazene-based flame retardant with active amine groups and its application in reducing the fire hazard of Epoxy Resin. *Journal of Hazardous Materials* 366:78–87
53. Lou G, Pei G, Wu Y, Lu Y, Wu Y, et al. 2021. Combustion conversion of wood to N, O co-doped 2D carbon nanosheets for zinc-ion hybrid supercapacitors. *Chemical Engineering Journal* 413:127502
54. Zhu W, Kim D, Han M, Jang J, Choi H, et al. 2023. Fibrous cellulose nanoarchitectonics on N-doped Carbon-based Metal-Free catalytic nanofilter for highly efficient advanced oxidation process. *Chemical Engineering Journal* 460:141593
55. Luo H, Rao W, Zhao P, Wang L, Liu Y, et al. 2020. An efficient organic/inorganic phosphorus-nitrogen-silicon flame retardant towards low-flammability epoxy resin. *Polymer Degradation and Stability* 178:109195
56. Song J, Chen C, Zhu S, Zhu M, Dai J, et al. 2018. Processing bulk natural wood into a high-performance structural material. *Nature* 554:224–28
57. Xiao L, Huang J, Wang Y, Chen J, Liu Z, et al. 2019. Tung Oil-based modifier toughening epoxy resin by sacrificial bonds. *ACS Sustainable Chemistry & Engineering* 7:17344–53
58. Wang X, Peng J, Zhang Y, Li M, Saiz E, et al. 2018. Ultratough bioinspired graphene fiber via sequential toughening of hydrogen and ionic bonding. *ACS Nano* 12:12638–45



Copyright: © 2023 by the author(s). Published by Maximum Academic Press on behalf of Nanjing Tech University. This article is an open access article distributed under Creative Commons Attribution License (CC BY 4.0), visit <https://creativecommons.org/licenses/by/4.0/>.